Simultaneous SAXS and WAXS Investigations of Changes in Native Cellulose Fiber Microstructure on Swelling in Aqueous Sodium Hydroxide

J. CRAWSHAW,[1] W. BRAS,[2] G. R. MANT,[2] R. E. CAMERON[1]

[1] University of Cambridge, Department of Materials Science and Metallurgy, New Museums Site, Pembroke Street, Cambridge, CB2 3QZ, United Kingdom

[2] CLRC Daresbury Laboratory, Daresbury, Warrington, Cheshire, WA4 4AD, United Kingdom

Received 27 November 2000; accepted 24 March 2001

ABSTRACT: Simultaneous small- and wide-angle X-ray scattering was used to follow changes in the microstructure of native cellulose (cellulose I) fibers during conversion to sodium cellulose I (Na-cellulose I) by aqueous sodium hydroxide. Wide-angle X-ray scattering was used to monitor the extent of conversion, while small-angle X-ray scattering was used to explore what occurs at the higher structural levels of the elementary fibrils, microfibrils, and interfibrillar voids. Native cellulose fibers, swollen in either water or aqueous sodium hydroxide, exhibited an increase in the void volume fraction and a decrease in the void cross-section size, as the swelling agent separated elementary fibrils, opening up the structure, and creating many small voids. After conversion of swollen native cellulose to sodium cellulose I, the void volume fraction and average void cross-section dimensions both increased. During conversion from dry cellulose I fibers to swollen Na-cellulose I fibers, the void cross-section dimensions went through a minimum, suggesting that the void structure may go via an intermediate similar to the water swollen structure of cellulose I. © 2002 John Wiley & Sons, Inc. J Appl Polym Sci 83: 1209–1218, 2002

Key words: bipolymers; fibers; polysaccharides; SAXS; WAXS

INTRODUCTION

When native cellulose is swollen in aqueous sodium hydroxide, washed in water, and dried, the crystal structure is transformed from cellulose I to cellulose II. In this process, referred to as "mercerization," the crystal structure transformation occurs in the solid state, and goes via a number of semicrystalline sodium cellulose intermediates. Okano and Sarko[1] used wide-angle X-ray scattering, WAXS, to characterize the sodium cellulose intermediates formed, and defined the first sodium cellulose structure as Na-cellulose I.

Chains in cellulose I are parallel packed.[2] However, some authors argue that cellulose II has an antiparallel packed structure.[3–5] The Na-cellulose I intermediate is also argued to be antiparallel packed[1] and so the transformation from cellulose I to Na-cellulose I may be regarded as a transformation from a parallel to an antiparallel structure. Because mercerization occurs in the solid state, there is limited scope for polymer

Correspondence to: R. E. Cameron (rec11@cam.ac.uk).

Journal of Applied Polymer Science, Vol. 83, 1209–1218 (2002)

DOI 10.1002/app.2287

chain rearrangement during transformation, and such a transformation is regarded as somewhat surprising. Sarko and coworkers[6–8] proposed a mechanism for the transformation of cellulose I to Na-cellulose I in which the original cellulose I is composed of parallel packed crystals in two populations pointing both up and down the fiber. During mercerization the chains reorganize into antiparallel crystals without the need for complete rotation of any given chain. They argue that small crystals and uncrystallized chains are rapidly converted first, followed by slower conversion of larger crystals.

Some authors question this mechanism on the basis that the chain rearrangements required are still too large to be feasible.[9] Other authors propose that the packing in cellulose II (and Na-cellulose I) is actually parallel, removing the need for large-scale chain rearrangement.[10,11]

In addition to the crystal structure, the larger scale fibrous structure of native cellulose[12–14] will also be affected by the interconversion, although the details of the effects are unknown. The fiber is composed of bundles of microfibrils, approximately 35–100 Å thick and 100–350 Å wide. The microfibrils are themselves composed of bundles of elementary fibrils, consisting of elementary crystallites, approximately 35 × 35 Å in cross section, separated by less ordered amorphous regions along the fiber axis direction. Each cellulose chain may pass through several elementary crystallites and amorphous regions, thus providing the elementary fibril with internal cohesion. Elongated voids, approximately 20 to 300 Å wide, occur between some of the fibrillar elements, at both the elementary fibrillar and microfibrillar structural levels.

Recently, the time dependence of the conversion of cellulose to alkali cellulose has been studied, by using synchrotron radiation to obtain WAXS patterns in real time during the reaction.[15]

The work reported here uses synchrotron radiation to make simultaneous SAXS and WAXS observations of native cellulose fibers as they were swollen in aqueous sodium hydroxide, NaOH(aq). The aim was to use WAXS to monitor the progress of the transformation from cellulose I to Na-cellulose I, while SAXS simultaneously provided information on changes at the higher structural levels of the elementary fibrils, microfibrils, and interfibrillar voids.

MATERIALS AND METHODS

The experimental apparatus incorporated a two-dimensional detector for both the SAXS and the WAXS on station 8.2 at the Daresbury Laboratory.[16] Time-resolved data were collected as ramie native cellulose fibers were swollen in water, 1.5 *M* NaOH(aq), 4 *M* NaOH(aq), 5 *M* NaOH(aq), and 6 *M* NaOH(aq). Data were collected for 25 min, in 15-s frames for the first 5 min, and 60 s frames for the remaining 20 min.

The water, or aqueous sodium hydroxide, was added to the fibers in the sample cell using an automatic syringe driver. A slow driver speed allowed the fibers exposed to the beam to remain dry until after the 1-min beam interlock procedure was completed and the X-ray shutter opened. In this way, we could collect data first from dry fibers, and then as they were swollen in the chosen medium.

The syringe driver was switched off after 5 min to prevent liquid overflowing the sample cell. Data collection was resumed after second interlock procedure resulting in a gap in the time resolved data, which was noted and included on the time axis of plots.

Data Analysis

In keeping with convention, the direction parallel to the fiber axis will be referred to as the "meridian," and the perpendicular direction will be referred to as the "equator."

The two-dimensional SAXS and WAXS data were corrected for variations in the incident beam intensity and nonuniformity of the detector response. A normalized background contribution of scattering from an empty sample cell was subtracted from normalized sample data. Where necessary, the images were rotated. The scattering angle was calibrated in both the meridional and equatorial directions using wet rat tail collagen for SAXS, and high-density polyethylene for WAXS.

WAXS Data Analysis

After the preliminary treatment, the WAXS data were reduced to one-dimensional equatorial curves of scattering angle vs. intensity. The positions of the equatorial WAXS peaks were estimated using the Daresbury software "Fit"[17] to fit

curves to the crystalline peaks and noncrystalline scatter.

SAXS Data Analysis

In a simple model, cellulose fibers may be treated as a two-phase system of void and crystalline cellulose, with the elementary fibrils being treated as strings of cellulose crystallites. This is valid because the noncrystalline regions of the fibrils are also highly oriented and, therefore, to a first approximation may be treated as crystalline. The degree of crystallinity for cellulose fibers is generally high, and was found from laboratory-based WAXS measurements to be typically ~70% for the ramie fibers used in these experiments. SAXS patterns collected from dry native cellulose fibers appeared as a diamond-shaped streak elongated on the equator. SAXS patterns from hydrated fibers were also centered on the equator, but extended further out on the meridian in places, giving the pattern a lobed shape. Furthermore, the hydrated fiber SAXS extended further out on the equator than in the dry fiber case. In both cases the elongation of the SAXS on the equator indicates long thin scattering particles oriented approximately parallel to the fiber axis (the meridian).

The SAXS patterns were integrated along the meridian (q_z) at fixed equatorial positions (q_x) to give an integrated equatorial intensity,

$$\tilde{I}(q_x) = \int_{-\infty}^{\infty} I(\mathbf{q}) dq_z \tag{1}$$

In all cases, the integrated equatorial intensity, $\tilde{I}(q_x)$, was extrapolated to low q_x using the Guinier method with a q_x range of 0.01 $Å^{-1} < q_x < 0.015$ $Å^{-1}$. None of the equatorial data went to sufficiently high q_x to reach the point at which the SAXS fell to a background level, or for Porod's law to be applied for a high q_x extrapolation.

The low q_x extrapolated integrated equatorial intensity was used to estimate calculate the scattering power, Q (in arbitrary units), mean void cross-section length, L_2, mean radius of gyration of the void cross section, R_3, and the mean void cross section area, S_3, after the method of Shioya and Takaku.[18] This is described in more detail in an earlier article.[19] For a two-phase system consisting of cellulose and a dilute phase of voids, independent particle scattering may be assumed, and so the volume fraction of voids is given by the scattering power, Q, and electron density difference, ρ, between the voids and cellulose:[20]

$$\nu \propto \frac{Q}{\rho^2} \tag{2}$$

where,

$$Q = \int_0^{\infty} \tilde{I}(q_x) q_x dq_x \tag{3}$$

When the voids are not dilute, independent particle scattering is not obtained and the void volume fraction is given by:

$$\nu(1 - \nu) \propto \frac{Q}{\rho^2} \tag{4}$$

In dry fibers the voids form a dilute phase and eq. (2) may be applied. However, for fibers swollen in water or NaOH(aq) the voids cannot be considered to form a dilute system, and eq. (4) must be used. Absolute intensities were not available; therefore, the proportionalities shown in (2) and (4) were used to track the direction of changes in the void fraction on swelling.

In dry fibers it is assumed that the voids are filled with air, while after swelling is complete it is assumed that the voids are filled with liquid of the appropriate electron density. This assumption has been justified in neutron scattering experiments described in an earlier article.[21] The density of cellulose is assumed to be constant throughout the experiment. The electron density differences between cellulose and the media used in this study are as follows: air, 850 N_A; water, 294 N_A; 1.5 *M* NaOH (aq), 264 N_A; 4 *M* NaOH(aq), 220 N_A; 5 *M* NaOH(aq), 200 N_A; 6 *M* NaOH(aq), 186 N_A.

L_2, R_3, and S_3 characterize the voids in the cross-section perpendicular to the fiber axis. The Guinier plot, used to calculate R_3 and S_3, will be a curve rather than a straight line, if there is a wide distribution of void sizes, or if the void cross-section shape is highly anisotropic, or both. The curve is the result of superposition of straight lines, each with a different gradient and intercept, each representing a different void size or shape. Two ranges of q_x were used to estimate the distribution of void sizes: 0.01 $Å^{-1} \leq q_x < 0.015$

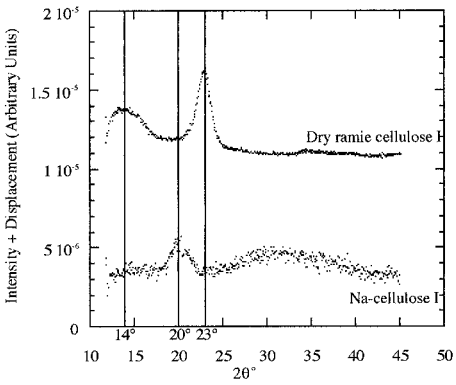

Figure 1 A comparison between equatorial WAXS from dry ramie and the same sample after swelling in 5 *M* NaOH(aq). The plot for each individual frame has been offset by adding a fixed displacement to the intensity.

$Å^{-1}$, which gives a measure of the size of larger voids in the structure, and a high q_x range, 0.015 $Å^{-1} < q_x < 0.06\ Å^{-1}$, which gives a measure of the size of smaller voids. Finally, a rectangular void cross section was assumed, and the average lengths of the sides of the voids X and Y calculated from the parameters R_3 and S_3. Such an analysis is not ideal, because the method is only truly valid if the Guinier plot is a straight line. However, this approach, applied consistently across the data, gives some measure of the changes in void size during the experiment.

Qualitative Assessment of the Accuracy of the SAXS Parameters

The swollen fiber equatorial SAXS data did not reach a background level, and they could not be extrapolated to high q_x because they were cut off part of the way through the interference peak. Therefore, the upper limit of the integrals used in calculating L_2, Q, and S_3 did not include the full q_x range of equatorial scattering. However, as the high q_x limit of the data was the same for all the data from a particular experiment, the inaccuracy introduced into the calculation of L_2, S_3, and Q was largely systematic. Therefore, although actual magnitudes of the void parameters cannot be accurately deduced, trends may be regarded as valid. As the dry fiber data reached a background level within the available q_x range, this source of systematic error does not apply for the dry fiber case.

Shioya and Takaku's[18] method for calculating void sizes from SAXS from oriented voids within uniaxially aligned fibers was derived assuming independent particle scattering from dilute packed voids. For dry cellulose fiber SAXS, this analysis is valid because of the low-volume fraction of voids.[22] However, closer packing of the voids in water or NaOH(aq) swollen cellulose fibers gives rise to interparticle interference. This changes the shape of the SAXS curve introducing a systematic error in the calculation of the void parameters. Hence, again general trends in changes of the void parameters will be regarded as valid, but magnitudes cannot be accurately deduced.

RESULTS AND DISCUSSION

Preliminary Observations on SAXS Data

Dry native cellulose fiber SAXS produced a diamond-shaped equatorial streak originating from long thin oriented voids. When all types of native cellulose fiber studied were swollen in either water or aqueous sodium hydroxide, the SAXS pattern broadened in the meridional direction becoming lobe shaped. This meridional broadening is consistent with two processes; the voids becoming misoriented with respect to the fiber axis, and

Table I Comparison of the Void Parameters and of Dry, Water Swollen, and 1.5 M NaOH (aq) Swollen Ramie Native Cellulose Fibers

Ramie Fibers	R_3 (Å)	L_2 (Å)	S_3 (Å^2)	$\frac{Q}{\rho^2} \times 10^{13}$ N$_A^2$
Dry	30–135	115	2000–30,000	5
Water swollen	15–70	45	1400–3000	95
1.5M NaOH(aq) swollen	10–85	45	1500–2500	100

Smaller values (calculated from the higher q range) of R_3 and S_3 are seriously affected by the interference peak in water and 1.5 M NaOH(aq) swollen fibers.

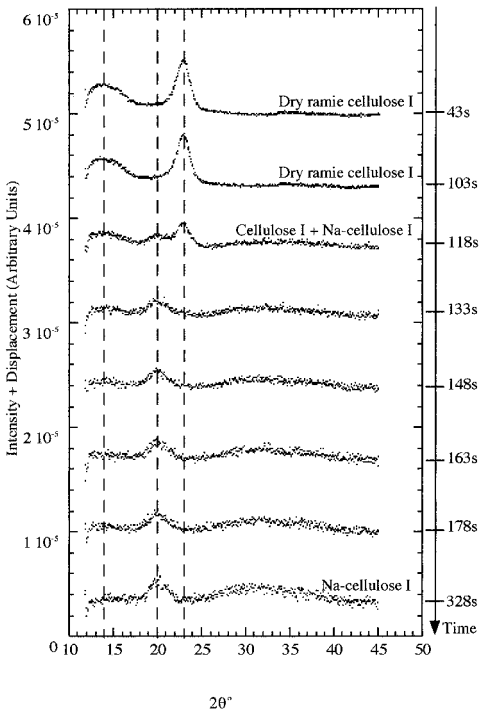

Figure 2 Time-resolved equatorial WAXS for ramie native cellulose fibers as they are swollen in 5 *M* NaOH(aq). The plot for each individual frame has been offset by adding a fixed displacement to the intensity.

shorter in that direction. The lobes became more rounded as the molarity of NaOH(aq) was increased, indicating increased misorientation and/or shortening of the voids.

As dry fibers were hydrated, the equatorial scatter extended to higher q. Moreover, when the cellulose I had been converted to Na-cellulose I, the equatorial scatter extended to still higher q. The equatorial scatter extends to higher q as the scattering particles narrow in the perpendicular direction (meridian). Therefore, the voids are widest in dry cellulose I , become narrower in hydrated cellulose I, and narrower still after conversion to Na-cellulose I.

Preliminary Observations WAXS Data

Dry fiber, and water or 1.5 *M* NaOH(aq) swollen fiber WAXS patterns, showed two clear peaks: a low broad peak centred at $2\theta \cong 14°$, which corresponds to an interplanar spacing of $d \cong 3.9$ Å ($\lambda = 1.54$ Å), and a higher sharper peak centred at $2\theta \cong 14°$, which corresponds to an interplanar spacing of $d \cong 6.3$ Å ($\lambda = 1.54$ Å). The higher peak probably corresponds to the (002) peak in cellulose I, and the lower broader peak probably corresponds to the superposition of the ($10\bar{1}$ and (101) peaks in cellulose I.[2]

Ramie, which had been steeped in NaOH(aq) of 4 *M* or above, exhibited a single crystalline peak at $2\theta \cong 20°$. This corresponds to an interplanar spacing of $d \cong 4.4$ Å ($\lambda = 1.54$ Å), and may be identified as the (200) peak of Na-cellulose I.[20] As an example, Figure 1 compares equatorial WAXS from dry and 5 *M* NaOH(aq) swollen ramie.

The peaks were quite broad, partly as a result of parallax due to the interaction depth of the detector. The parallax broadening causes misshaped peaks. Other causes of the broad crystalline peaks are the finite sizes of the cellulose crystallites and imperfections in the crystals. In addition, the superposition of peaks in the case of the measured peak at $2\theta \cong 14°$ will add to the broadening.

The Structure of Dry, Water-Swollen, and 1.5 *M* NaOH(aq)-Swollen Ramie Fibers

The WAXS results indicate that the cellulose crystal structure in dry, water-swollen, and 1.5 *M*

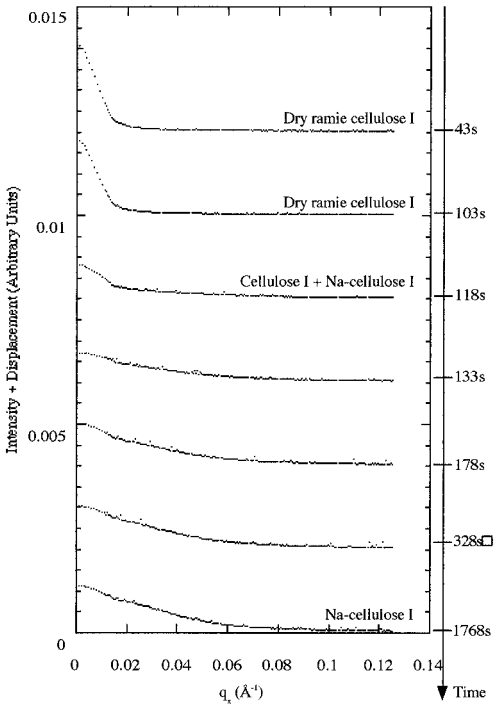

Figure 3 Time-resolved integrated equatorial SAXS for ramie cellulose I fibers swelling in 5 *M* NaOH(aq). The plot for each individual frame has been offset by adding a fixed displacement to the intensity.

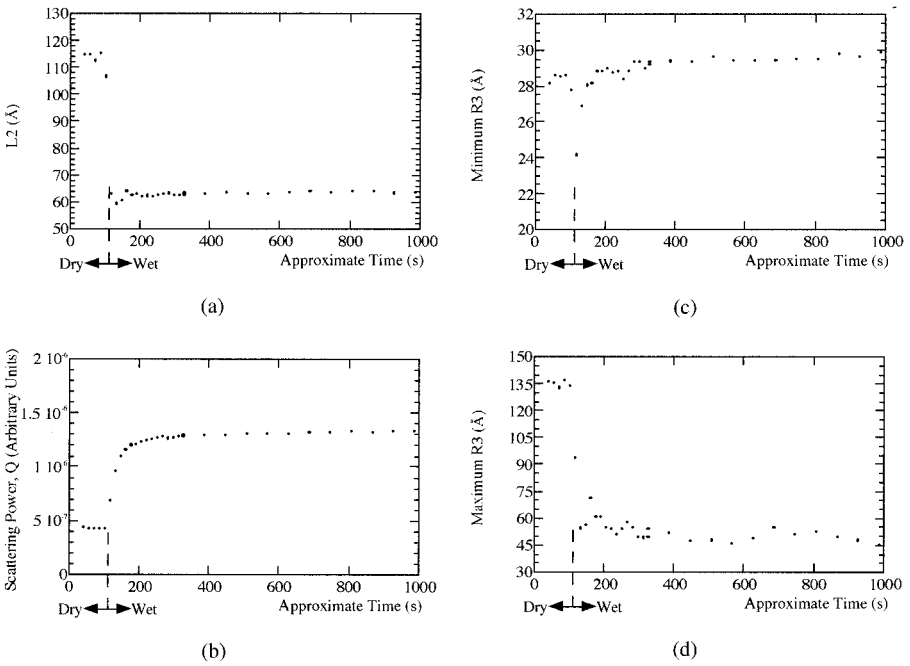

Figure 4 Changes in the mean void parameters as ramie fibers swell in 5 *M* NaOH: (a) mean void cross section length, L_2; (b) scattering power, Q; (c) smaller value (from the high q range) value of the radius of gyration of the void cross section, R_3; (d) larger value (from the low q range) value of the radius of gyration of the void cross section, R_3; (e) smaller value (from the high q range) value of the void cross-section area, S_3; (f) larger value (from the low q range) value of the void cross section area, S_3; (g) smaller value (from the high q range) values of rectangular void cross section dimensions, X and Y; and (h) larger value (from the low q range) values of rectangular void cross-section dimensions, X and Y.

NaOH(aq)-swollen ramie fibers was the cellulose I allomorph. Hence, in these samples, no crystalline transformation occurred during swelling. The void parameters, Q/ρ^2, L_2, R_3, and S_3, calculated from the corresponding SAXS patterns for dry ramie fibers, are listed in Table I.

The fiber cross-section void parameters are larger in dry fibers than in swollen fibers, and there is a greater difference between the two values of radius of gyration calculated. The void volume fraction, proportional to Q/ρ^2, is approximately 20 times lower in dry fibers. This indicates that dry ramie native cellulose fibers contain few voids, and those that are present, appear in a wide range of cross-section sizes. Upon swelling, the void volume fraction increases dramatically, and the mean cross-section sizes are lower and have a narrower size range than in dry fibers. These trends are similar to those reported elsewhere,[18] although exact values may differ because of the chosen q-range and lack of high q extrapolation.

The void parameters for ramie fibers swollen in 1.5 *M* NaOH(aq) were broadly the same as those for water-swollen fibers, within the accuracy of the data, suggesting that water and 1.5 *M* NaOH(aq) are very similar swelling agents for cellulose I.

Results of Time-Resolved Observations of Mercerization of Ramie in 5 *M* NaOH(aq)

Figure 2 shows a set of time-resolved equatorial WAXS scattering plots for ramie native cellulose fibers during swelling in 5 *M* NaOH(aq). The first five frames were for dry ramie, the first (43 s) and fifth (103 s) frames are shown, and the equatorial WAXS peak positions correspond to those for the cellulose I crystal structure. After the fifth frame, the 5 *M* NaOH(aq) reached the fibers within the beam, which started to swell. That swelling started at this stage was also evident from the two-dimensional SAXS data, which started to broaden in the meridional direction. The conver-

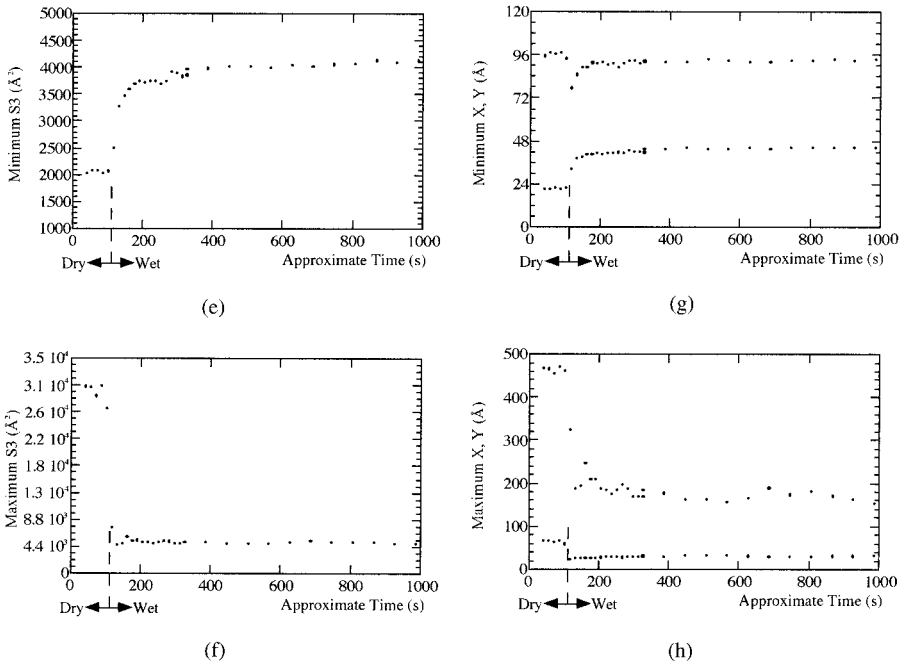

Figure 4 (*Continued from the previous page*)

sion to Na-cellulose I started immediately as the fibers began to swell; this was shown by the appearance of the Na-cellulose I peak at $2\theta = 20°$ alongside the cellulose I peaks in the sixth frame, recorded after 118 s. From the seventh frame, recorded after 133 s, the cellulose I peaks could not be clearly distinguished, indicating that a high proportion of the cellulose I crystallites had been converted to Na-cellulose I. Therefore, it appears that in 5 *M* NaOH(aq) the majority of cellulose I was rapidly converted to Na-cellulose I, within approximately 30 s, between the fifth and seventh frames. This is consistent with the findings of Fink et al.[15] from WAXS measurement, which also suggested that conversion proceeds rapidly.

Figure 3 shows the simultaneously collected time resolved integrated equatorial SAXS for ramie cellulose fibers after swelling in 5 *M* NaOH(aq). The integrated equatorial SAXS data show a decrease in low-angle intensity as the dry ramie cellulose I was swollen in 5 *M* NaOH(aq), and partially converted to Na-cellulose I, between the fifth and sixth frames, recorded after 103 s and 118 s. The void parameters, L_2, Q, R_3, S_3, and X, Y, calculated from the integrated equatorial SAXS, all show variation over approximately the first 12 frames recorded up to 208 s. These void parameters are plotted as a function of time in Figure 4(a)–(f). No clear SAXS interference peak was observed in the NaOH(aq) swollen fibers, which underwent conversion. This suggests that smaller values (i.e., those calculated from the high q range) of R_3 and S_3 will be more reliable for these samples, than for the wet samples where a peak was observed.

Overall, L_2 and the larger value (from the low q range) cross-section void parameters R_3, S_3, X, and Y, all decreased as the ramie fibers were swollen in 5 *M* NaOH(aq). The smaller value (from the high q range) void parameters stayed constant, or increased, thus narrowing the range of void cross-section sizes in 5 *M* NaOH(aq) swollen fibers compared with dry or water-swollen fibers. These changes in the cross-section void parameters were accompanied by an approximate doubling of the scattering power, Q. When the relative estimated electron density differences between air filled voids and 5 *M* NaOH(aq) filled voids are taken into account, this increase implies a much larger increase in the void volume fraction.

The smaller value (from the high q range) of R_3 exhibited a dip when the 5 *M* NaOH(aq) was first added to the fibers. This dip is rather small to be considered significant within the accuracy of the

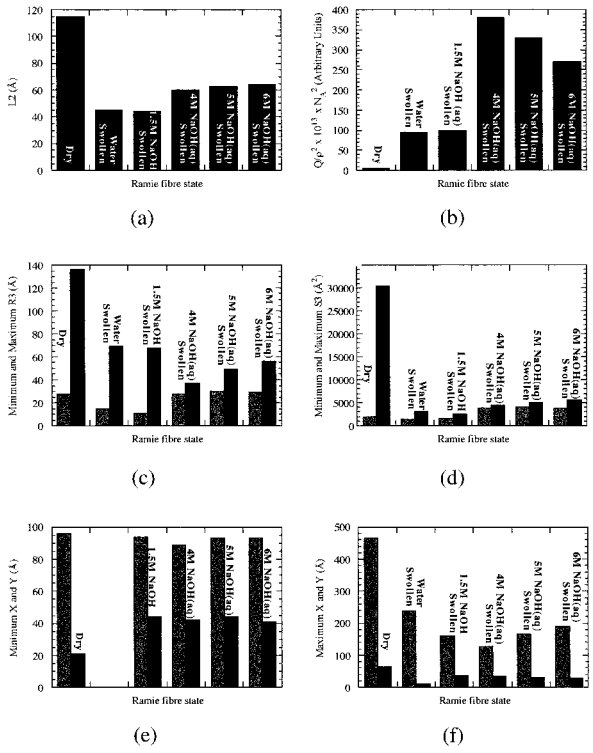

Figure 5 Mean void parametrs of dry, water-swollen, and NaOH-swollen ramie fibers: (a) mean void cross section length, L_2; (b) void fraction product, Q/ρ^2; (c) larger value (from the low q range) and smaller value (from the high q range) values of the radius of gyration of the void cross section, R_3; (d) larger value (from the low q range) and smaller value (from the high q range) values of the void cross section area, S_3; (e) smaller value (from the high q range) values of rectangular void cross-section dimensions, X and Y; and (f) larger value (from the low q range) values of rectangular void cross-section dimensions, X and Y.

data. However, it also appeared for the other concentrations of NaOH used, and is likely to be real. Small dips are also seen in L_2, X, and$Y$, and which again, although noisy, are almost certainly real.

The Effect of Aqueous Sodium Hydroxide Concentration

The changes in L_2, Q, R_3, S_3, and X, Y as fibers were swollen, and cellulose I was converted to Na-cellulose I, followed the same pattern when swollen in 4 M and 6 M NaOH(aq). The changes occurred more quickly the higher the molarity with the 4 M sample, displaying a mixed WAXS pattern for nearly 200 s. Figure 5(a)–(f) show histograms of the void parameters calculated for dry, water-swollen, and NaOH(aq)-swollen fibers. The values displayed are the means of values for frames at the start and end of data collection over which no change in the equatorial SAXS and WAXS was evident.

Interpretation of Time-Resolved Simultaneous SAXS and WAXS Observations of Dry, Water, and NaOH(aq)-Swollen Ramie Fibers

The reduction in void cross-section size observed when dry ramie fibers were swollen in water or aqueous sodium hydroxide can be explained by the swelling agent separating elementary fibrils, or groups of elementary fibrils, thereby opening up the structure, and creating many small voids. This accounts for the increase in void volume fraction on swelling, as smaller voids, which were collapsed in the dry fibers, open up on filling liquid. On swelling, the large voids in the dry fibers disappear as crystallites, interspersed by small voids, move into the large void space. Figure 6 is a schematic illustration of the changes, described above, in the arrangement of voids and crystallites in the ramie cellulose fibers as they are swollen.

Comparison between water, or 1.5 M NaOH(aq), swollen ramie native cellulose fibers, and 5 M NaOH(aq) swollen fibers composed of Na-cellulose I crystallites, indicated that both void volume fraction and cross-section size are larger for the fibers swollen in the 5 M NaOH(aq). It is significant that water and 1.5 M NaOH(aq) swollen fibers have almost identical void parameters. In both cases the crystal structure remains entirely cellulose I; therefore, changes observed are due to the fibers swelling in a polar liquid. When the ramie native cellulose fibers are swollen in the 5 M NaOH(aq), the swelling is accompanied by a change of crystal structure from cellulose I to Na-cellulose I. Figure 6 is a schematic comparison between water and 5 M NaOH(aq) swollen ramie fiberes.

The dips seen in L_2 and the smaller values (calculated from the high q range) of R_3 on swelling in 5 M NaOH(aq) suggest that the structure may go via an intermediate, similar to the water-swollen structure, before conversion to the fiber structure containing Na-cellulose I. Such a structure might be associated with the first stage of Sarko and coworkers' model[6,8] in which small crystals and aligned amorphous chains rearrange and transform, and which might be expected to

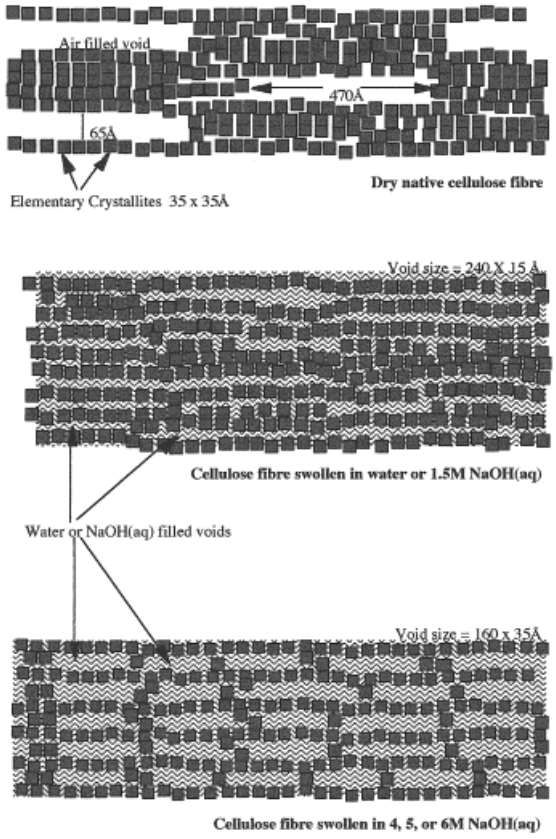

Figure 6 Schematic illustration of changes to the voids within native cellulose fibers as during swelling in water, or 1.5 *M* NaOH(aq), and 4, 5, or 6 *M* NaOH(aq). View in plane perpendicular to fiber axis.

give a more finely divided pore structure. Equally, it could be associated with a preliminary swelling stage, before bulk conversion takes place, and need not be associated with the large-scale chain rearrangements of Sarko et al.'s model. The data could, therefore, be consistent with a transformation from a parallel to antiparallel structure on mercerization, but does not provide any evidence for or against this.

The molarity of aqueous sodium hydroxide in the range 4 to 6 molar appears to have little effect on the final swollen fiber cross-section void sizes and the void volume fraction, but the changes are faster the higher the molarity.

CONCLUSIONS

SAXS results demonstrated that dry native cellulose ramie fibers contain a small number of relatively large voids (~100 Å wide). The overall shape of the SAXS is due to the voids being long, thin, and oriented, with their long axis approximately parallel to the fiber axis.

When the ramie native cellulose fibers were swollen in water or NaOH(aq), the void volume fraction increased and the void cross-section size decreased as the swelling agent separated elementary fibrils, or groups of elementary fibrils, opening up the structure, and creating many small voids.

Both the void volume fraction and the average void cross-section size were found to be greater after conversion to Na-cellulose I. During conversion some of the cross section void parameters passed through minima, suggesting that the void structure may go via an intermediate similar to the water-swollen structure.

The authors are grateful to Courtaulds Corporate Technology (now part of the Akzo Nobel group) for financial support, and to the EPSRC for funding. The X-ray experiments were performed on station 8.2 at the Daresbury laboratory.

REFERENCES

1. Okano, T.; Sarko, A. J Appl Polym Sci 1984, 29, 4175.
2. Woodcock, C.; Sarko, A. Macromolecules 1980, 13, 3.
3. Sarko, A.; Muggli, R.. Macromolecules 1974, 7, 4.
4. Kolpak, F. J.; Blackwell, J. Macromolecules 1976, 9, 2.
5. Stipanovic, A. J.; Sarko, A. Macromolecules 1976, 9, 5.
6. Okano, T.; Sarko, A. J Appl Polym Sci 1985, 30, 325.
7. Nishimura, H.; Sarko, A. J Appl Polym Sci 1987, 33, 855.
8. Nishimura, H.; Sarko, A. J Appl Polym Sci 1987, 33, 867.
9. Turbak, A. F.; Sakthivel, A. Chemtech 1990, 444.
10. Maurer, A.; Fengel, D. Holzals Roh Werkstoff 1992, 50.
11. Kroon-Batenburg, L. M. J.; Bouma, B.; Kroon, J. Macromolecules 1996, 29, 5695.
12. Young, R. A. In Cellulose, Structure, Modification, and Hydrolysis; Young, R. A.; Rowell, R. M., Eds.; John Wiley & Sons, Inc.: New York, 1986, Chap. 6.
13. Preston, R. D. In Cellulose, Structure, Modification, and Hydrolysis; Young, R. A.; Rowell, R. M., Eds.; John Wiley & Sons, Inc.: New York, 1986, Chap. 1.

14. Yachi, T.; Hayashi, J.; Takai, M.; Shimizu, Y. J Appl Polym Sci Appl Polym Symp 1983, 37, 325.
15. Fink, H. P.; Walenta, E.; Philipp, B. Papier 1999, 53, 25.
16. Bras, W.; Mant, G. R.; Derbyshire, G. E.; Ryan, A. J.; O'Kane, W. J.; Helsby, W. I.; Hall, C. J. J Synchrotron Radiat 1995, 2, 87.
17. Denny, R. Fit, Daresbury peak fitting software, CCP13.
18. Shioya, M.; Takaku, A. J Appl Phys 1985, 58, 11.
19. Crawshaw, J.; Cameron, R. E. Polymer 2000, 41, 4691.
20. Porod, G. In Small Angle X-ray Scattering; Glatter, O.; Kratky, O., Eds.; Academic Press: New York, 1982, Chap. 2.
21. Crawshaw, J.; Vickers, M. E.; Briggs, N. P.; Heenan, R. K.; Cameron, R. E. Polymer 2000, 41, 1873.
22. Statton, W. O. J Polym Sci 1956, 22, 385.
23. Nishimura, H.; Okano, T.; Sarko, A. Macromolecules 1991, 24, 759.